



Published in final edited form as:

Vet Immunol Immunopathol. 2016 December ; 182: 150–158. doi:10.1016/j.vetimm.2016.10.014.

Porcine Treg depletion with a novel diphtheria toxin-based anti-human CCR4 immunotoxin

Zhaohui Wang^a, Nalu Navarro-Alvarez^a, Jigesh A. Shah^a, Huiping Zhang^a, Qi Huang^a, Qian Zheng^a, Joren C. Madsen^{a,c}, David H. Sachs^{a,b}, Christene A. Huang^{a,*}, and Zhirui Wang^{a,*}

^aCenter for Transplantation Sciences, Massachusetts General Hospital and Harvard Medical School, Boston, Massachusetts, USA

^bTBRC Laboratories, Center for Transplantation Sciences, Massachusetts General Hospital and Harvard Medical School, Boston, Massachusetts, USA

^cDivision of Cardiac Surgery, Massachusetts General Hospital and Harvard Medical School, Boston, Massachusetts, USA

Abstract

Regulatory T cells (Tregs) are known to play an important role in immunoregulation and have been shown to facilitate induction of transplantation tolerance. Chemokine (C-C motif) receptor 4 (CCR4) is expressed on the surface of effector Tregs involved in controlling alloimmune and autoimmune responses. Recently we have developed a novel diphtheria-toxin based anti-human CCR4 immunotoxin for depleting CCR4⁺ cells *in vivo*. In this study, we have demonstrated that the anti-human CCR4 immunotoxin bound to porcine lymphocytes including CD4⁺FoxP3⁺ Tregs. Anti-human CCR4 immunotoxin effectively depleted CCR4⁺ Foxp3⁺ porcine Tregs *in vivo*. We observed depletion of up to 70–85% of the CCR4⁺Foxp3⁺ porcine Tregs in the peripheral blood and 85–91% in the lymph nodes following the anti-human CCR4 immunotoxin treatment in Massachusetts General Hospital (MGH) miniature swine. The depletion lasted for about one week with no significant reduction observed within CCR4[−] cell populations including CD8α⁺ T cells, CCR4[−]CD4⁺ T cells and B cells. In summary, anti-human CCR4 immunotoxin effectively depleted CCR4⁺Foxp3⁺ porcine Tregs in both peripheral blood and lymph nodes.

Keywords

porcine Treg; CCR4; immunotoxin; diphtheria toxin; MGH miniature swine

*Corresponding authors: Zhirui Wang, Ph.D., Center for Transplantation Sciences, Massachusetts General Hospital and Harvard Medical School, MGH-East, Building 149-6113, 13th Street, Boston, MA 02129, USA, Phone: +1-617-643-1957; Fax: +1-617-726-4067, zwang7@mgh.harvard.edu. Christene A. Huang, Ph.D., Center for Transplantation Sciences, Massachusetts General Hospital and Harvard Medical School, MGH-East, CNY149-9019, 13th Street, Boston, MA 02129, USA, Phone: +1-617-726-6505; Fax: +1-617-726-4067, cahuang@mgh.harvard.edu.

Publisher's Disclaimer: This is a PDF file of an unedited manuscript that has been accepted for publication. As a service to our customers we are providing this early version of the manuscript. The manuscript will undergo copyediting, typesetting, and review of the resulting proof before it is published in its final citable form. Please note that during the production process errors may be discovered which could affect the content, and all legal disclaimers that apply to the journal pertain.

1. Introduction

Porcine regulatory T cell (Treg) phenotype and function was first described in 2008 (Kaser et al., 2008a). Similar to human Tregs, CD4⁺Foxp3⁺ T cells were defined as the marker of porcine Tregs (Kaser et al., 2008a, 2008b). Porcine Tregs were shown to suppress proliferation of porcine T-helper cells, cytotoxic T lymphocytes and TCR- $\gamma\delta$ T cells. Suppression was mediated through cell-cell direct contact, soluble components and/or competition for growth factors (Kaser et al., 2011, 2012). Porcine CD8 α ⁺Foxp3⁺ Tregs (either CD4⁺ or CD4⁻) were also identified (Kaser et al., 2008b; Talker et al., 2013). Porcine iTregs could be induced *in vitro* by CD3-stimulation in the presence of IL-2 and TGF- β (Kaser et al., 2015).

Major histocompatibility complex (MHC)-defined, Massachusetts General Hospital (MGH) miniature swine provide a unique preclinical large animal model for studies of immune regulation and transplantation tolerance. Although Tregs have been reported to be involved in swine models of allograft tolerance (Griesemer et al., 2008; Avsar et al., 2016) their precise role in transplantation tolerance induction and maintenance is not yet clear. The lack of an effective reagent available to deplete porcine Tregs *in vivo* has hindered the ability to investigate the mechanism further in swine. CCR4 is expressed on majority of effector Tregs and is a promising target for depleting effector Tregs (Sugiyama et al., 2013). Recently, we have developed a novel diphtheria toxin-based anti-human CCR4 immunotoxin using unique diphtheria toxin-resistant yeast *Pichia Pastoris* expression system (Wang et al., 2015). *In vivo* efficacy for targeting human CCR4⁺ tumors was characterized using human CCR4⁺ tumor-bearing NOD/SCID IL-2 receptor $\gamma^{-/-}$ (*NSG*) mouse model (Wang et al., 2015) and *in vivo* efficacy for targeting CCR4⁺ Tregs was characterized using two naive cynomolgus monkeys (Wang et al., 2016). In the current study, we demonstrate cross-reactivity of this reagent to swine CCR4 and demonstrate its efficacy to deplete CCR4⁺Foxp3⁺ porcine Tregs in two naive MGH miniature swine.

2. Materials and methods

2.1. Antibodies and immunotoxins

Antibodies used in this study are listed in Table 1. The monovalent, bivalent and single-chain foldback diabody anti-human CCR4 immunotoxins as well as DT390 alone were produced in our lab using unique diphtheria toxin resistant yeast *Pichia Pastoris* expression system (Wang et al., 2015) and biotinylated as previously described (Wang et al., 2015).

2.2. In vitro binding and depletion analysis

To perform the *in vitro* binding analysis of the anti-human CCR4 immunotoxins to porcine blood cells by flow cytometry, porcine whole blood was stained with the biotinylated anti-human CCR4 immunotoxin as primary staining and PE-conjugated streptavidin as secondary staining. Porcine whole blood with only the secondary staining (PE-conjugated streptavidin) served as the negative control and PE-mouse anti-human/rat CCR4 mAb (clone# 205410) as the CCR4 positive control, PE-mouse IgG2B (clone# MPC-11) for the isotype control of PE-mouse anti-human/rat CCR4 mAb (clone# 205410), PerCp-Cy5.5-mouse anti-pig CD4a

mAb (clone#74-12-4) as CD4 positive control. Biotin-labeled porcine CD3- $\epsilon\gamma$ (Peraino et al., 2012) was included as a negative control for background due to protein biotinylation. The stained samples were analyzed using BD FACSCalibur (BD Biosciences, San Jose, CA). To perform the *in vitro* binding analysis of the anti-human CCR4 immunotoxins to the CD4⁺ Foxp3⁺ porcine PBMC by flow cytometry, porcine PBMC was stained with FITC-rat anti-mouse Foxp3 mAb (clone# FJK-16s) and biotinylated anti-human CCR4 immunotoxin. Porcine PBMC with only the secondary staining (PE-conjugated streptavidin) served as the negative control, PE-mouse anti-human/rat CCR4 mAb (clone# 205410) as the CCR4 positive control, PE-mouse IgG2B (clone# MPC-11) for the isotype control of PE-mouse anti-human/rat CCR4 mAb (clone# 205410), PerCp-Cy5.5-mouse anti-pig CD4a mAb (clone#74-12-4) as CD4 positive control. FITC-rat anti-mouse Foxp3 mAb (clone# FJK-16s) was used for the Foxp3 positive control, FITC-rat-IgG2a, κ (clone# eBR2a) for the isotype control of FITC-rat anti-mouse Foxp3 mAb (clone# FJK-16s). Biotin-labeled porcine CD3- $\epsilon\gamma$ (Peraino et al., 2012) was included as a negative control for background due to protein biotinylation. The stained samples were analyzed using BD FACSCalibur (BD Biosciences, San Jose, CA). To perform the *in vitro* depletion analysis of the CCR4⁺ cells within porcine PBMC using the anti-human CCR4 immunotoxins, porcine PBMC were incubated with the unlabeled anti-human CCR4 immunotoxin at 37°C for 18 h and analyzed by flow cytometry using PE anti-human CCR4 mAb (clone# L291H4). Since the anti-human CCR4 immunotoxin was constructed using the scFv of the parent anti-human CCR4 mAb (clone 205410), another anti-human CCR4 mAb (clone L291H4) recognizing a different epitope was used for *in vitro* and *in vivo* depletion analysis. PE anti-human CCR4 antibody (clone # L291H4) was used as the CCR4 positive control, PE-mouse IgG1, κ (clone# MOPC-21) as isotype control of PE-anti-human CCR4 mAb (clone# L291H4), FITC-mouse anti-pig CD4a mAb (clone# 74-12-4) as the CD4 positive control and DT390 (100 nM) was included as a negative control for depletion. Propidium iodide was added to exclude dead cells prior to acquisition. All control cells were also incubated at 37°C for 18 h.

2.3. In vivo porcine Treg depletion

Two MGH miniature swine (23288: 16.4 kg, 3-month-old; 23290: 16.9 kg, 3 month-old) were maintained in MGH facility. MGH is an AAALAC (Association for Assessment and Accreditation of Laboratory Animal Care) accredited institute. All experiments were conducted with the approved MGH IACUC protocol (2014N000087). A central intravenous (IV) catheter was placed for immunotoxin injection and blood collection. The foldback diabody anti-human CCR4 immunotoxin was IV bolus injected at 50 $\mu\text{g/kg}$, BID for four consecutive days, 6 hours apart. The line was flushed by injecting 5 mL of heparin saline after the immunotoxin injection. The blood was collected daily for flow cytometry analysis in the first week and twice weekly thereafter. The animals were closely monitored twice daily during the immunotoxin injection and once daily after the immunotoxin treatment for any adverse effects. Clinical assessments for adverse events include daily clinical observation and complete blood counts. The animals were weighed weekly.

Porcine Treg and other cell populations in peripheral blood were measured at two time-points before the immunotoxin administration to obtain a baseline. Following immunotoxin administration, peripheral blood flow cytometry was performed daily for the first week and

twice weekly thereafter to monitor the effect of the immunotoxin treatment on all peripheral blood cell populations including T cells, B cells, NK cells, and monocytes.

Lymph node biopsies were performed prior to the immunotoxin injection on day -5 (Animal#23288) or day -3 (Animal#23290) and after the immunotoxin administration on day 4. Animal was sedated through indwelling line and intubated via general endotracheal anesthesia. A left paraumbilical incision was made, the fascia was incised and the abdomen was cautiously entered. The small bowel was eviscerated and two mesenteric lymph nodes were excised. The abdomen was closed with running 2-0 polydioxane suture for the fascia and 3-0 vicryl for the subcutaneous tissue. The skin was approximated with staples. A dry sterile dressing and fentanyl patch as well as a jacket was placed. The animal was extubated and taken to the cage for full recovery. Treg depletion in the lymph node was monitored by flow cytometry.

2.4. Flow cytometry analysis

Surface staining and flow cytometry analysis using porcine whole blood and BD FACS lysing solution was performed as described (Wang et al., 2016). Intracellular staining was performed to detect porcine Foxp3 as described (Wang et al., 2016). 20,000 events (lymphocytes or PBMC) for each sample were collected using BD FACSCalibur (BD Biosciences, San Jose, CA).

A combination of CD4, CCR4, CD45RA, Foxp3 was used to monitor the Treg populations in the porcine peripheral blood (CCR4⁺ cell: CD4⁺CCR4⁺; CCR4⁺ Treg: CCR4⁺Foxp3⁺ among the gated CD4⁺ cells; Effector-type Treg: CD45RA⁻Foxp3⁺ among the gated CD4⁺ cells). The off-target depletion effect on CCR4⁻ cell populations in the peripheral blood was monitored by flow cytometry using antibodies against CD3, CD4, CD8α, γδ, CD1, CD21, CD16, CD172a (CD4⁺ T cell: CD3⁺CD4⁺; CD8α⁺ T cell: CD3⁺CD8α⁺; γδ⁺ T cells: CD3⁺γδ⁺; CD1⁺ or CD21⁺ B cell: CD3⁻CD1⁺ or CD3⁻CD21⁺; NK cell: CD16⁺CD8α⁺; Monocyte: CD16⁺CD172a⁺). PBMC gating was performed for the monocyte analysis and lymphocyte gating was performed for the analysis of the other subsets. Treg depletion in the lymph node was monitored by flow cytometry using the antibodies against CD4, CCR4, CD45RA and Foxp3 (CCR4⁺ cell: CD4⁺CCR4⁺; CCR4⁺ Treg: CCR4⁺Foxp3⁺ among the gated CD4⁺ cells; Effector-type Treg: CD45RA⁻Foxp3⁺ among the gated CD4⁺ cells). The off-target depletion in the lymph node was monitored by flow cytometry using antibodies against CD3, CD4, CD8α, CD21 (CD4 T cell: CD3⁺CD4⁺; CD8α T cell: CD3⁺CD8α⁺; B cell: CD3⁻CD21⁺).

3. Results

3.1. In vitro binding and depletion analysis of the CCR4 immunotoxin to porcine blood cells or PBMC

To assess whether the anti-human CCR4 immunotoxin cross-reacts with CCR4⁺ porcine blood cells, we performed *in vitro* binding and depletion analysis. All three versions of the biotinylated anti-human CCR4 immunotoxins (monovalent, bivalent and foldback diabody) bound to CCR4⁺ porcine blood cells in a dose-dependent fashion with the foldback diabody

isoform demonstrating the strongest binding affinity, followed by the bivalent isoform and then the monovalent isoform (Fig. 1A). These results are consistent with the previous binding analysis performed with human CCR4⁺ CCRF-CEM leukemia cell line, human and monkey PBMC (Wang et al., 2015, 2016). *In vitro* depletion assays demonstrated a dose-dependent depletion of CCR4⁺ porcine PBMC with the foldback diabody version showing the most efficacy (Fig. 1B). Next, the binding affinity of the CCR4 immunotoxins to CCR4⁺ Foxp3⁺ Tregs in PBMC was assessed. The immunotoxins bound to the CCR4⁺Foxp3⁺ Tregs within porcine PBMC in a dose dependent manner, and again with the foldback diabody isoform showing stronger binding compared to the other two isoforms (Fig. 1C).

3.2. In vivo porcine Treg depletion with the CCR4 immunotoxin

In vivo porcine CCR4⁺ Treg depletion was performed in two naive MGH miniature swine. Based on our previous data (Wang et al., 2015, 2016) as well as the *in vitro* binding and depletion data in this study (Fig. 1A–C), foldback diabody CCR4 immunotoxin was chosen for the *in vivo* porcine CCR4⁺ Treg depletion. The CCR4 immunotoxin was administered intravenously at a dose of 50 µg/kg, BID, 6 hours apart for 4 consecutive days. This dosing strategy was chosen based on our previous experience with another recombinant diphtheria toxin based immunotoxin that targets porcine CD3⁺ T cells *in vivo* (Wang et al., 2011). The CD3 immunotoxin was constructed in a similar fashion as the CCR4 immunotoxin with the DT390 domain being identical for both. This dosing strategy using CD3 immunotoxin demonstrated efficacy while showing minimal toxicity (Wang et al., 2011). Depletion of porcine CCR4⁺ Tregs was monitored by flow cytometry. With the described dosing strategy, up to 90–97% depletion of porcine CCR4⁺ cells in the peripheral blood was achieved and the depletion lasted for approximately one week (Fig. 2A–B). In the peripheral blood, 70–85 % of CCR4⁺Foxp3⁺ Tregs were depleted with similar duration (Fig. 2C–D). Other cell populations including CD8α⁺ T cells, other CD4⁺ T cells and B cells were not affected (Fig. 2F, H–I). Approximately 86–90% of porcine CCR4⁺ cells and 85–91% of porcine CCR4⁺Foxp3⁺ Tregs were depleted from the lymph nodes after the four-day course of the immunotoxin treatment (Fig. 3A–C). Consistent with the peripheral blood analysis, other cell populations (CD8α⁺ T cells, CD21⁺ B cells and other CD4⁺ T cells) in the lymph nodes were not affected (Fig. 3B–C). Taken together, porcine CCR4⁺Foxp3⁺ Tregs were effectively depleted *in vivo* from both peripheral blood and lymph nodes by the foldback diabody anti-human CCR4 immunotoxin. To the best of our knowledge, this is the first effective agent for porcine CCR4⁺ Treg depletion *in vivo*.

As shown in Fig. 2E and 3B, CD45RA⁺Foxp3⁺ porcine Tregs were depleted less well than CCR4⁺Foxp3⁺ porcine Tregs in both peripheral blood and lymph nodes. In order to explore the possible reason, we have analyzed the expression profile of Foxp3 versus CD45RA and CCR4 versus CD45RA among the gated CD4⁺Foxp3⁺ porcine Tregs (Fig. 4). The data demonstrated that only approximately 45% of the CD45RA⁺Foxp3⁺ porcine Tregs are CCR4 positive, which explained why CD45RA⁺Foxp3⁺ porcine Tregs were depleted less well than CCR4⁺Foxp3⁺ porcine Tregs.

Discussion

Clinically, the animals were healthy without any adverse effects during the entire course of immunotoxin treatment. However, both animals developed line infections by the end of the study. As shown in Fig. 2D, the number of CCR4⁺Foxp3⁺ Tregs increased up to 3-fold relative to the pretreatment level after stopping the CCR4 immunotoxin administration. We did not observe this phenomenon in monkey Treg depletion study using the same CCR4 immunotoxin (Wang et al., 2016). We speculate that the rebound of the CCR4⁺Foxp3⁺ porcine Tregs may have contributed to an increased susceptibility to infection in these animals. Additional studies will need to be performed to confirm these findings.

The entire lymphocyte population significantly decreased during the course of the CCR4⁺ porcine Treg depletion (Fig. 2L) as observed in the monkey Treg depletion study (Wang et al., 2016). This transient lymphopenia is a possible functional indication of the CCR4⁺ porcine Treg depletion (Molledo et al., 2014). We speculate that this transient lymphopenia may have contributed to the decrease in absolute number of the CCR4 negative subsets (right panels of Fig. 2F–H). Interestingly, similar to what we observed in monkeys (Wang et al., 2016), the CCR4 immunotoxin had an inverse effect on porcine NK cells and monocytes (left panels of Fig. 2J–K) both of which expanded as CCR4⁺Foxp3⁺ porcine Treg were depleted. We speculate that the NK and monocyte expansion was triggered by decreasing Treg suppression to the maturation of NK and monocytes (Mayer et al., 2014). The NK and monocyte expansion are also possible functional indication of the CCR4⁺ porcine Treg depletion.

Precisely speaking, our *in vitro* flow cytometry binding data demonstrated that the biotinylated anti-human CCR4 immunotoxin bound to the porcine leukocytes (Fig. 1A). However, the more detailed flow cytometry analysis including CD4⁺ Foxp3⁺ data presented in this study (Fig. 1A and C, Fig. 2A and C) suggest that this population is most likely the porcine CCR4⁺ counterpart since the profiles are similar to that observed in human and monkey blood samples (Wang et al., 2015, 2016).

Supplementary Material

Refer to Web version on PubMed Central for supplementary material.

Acknowledgments

We would like to thank James A. Winter and Sarah Lofgren for technical assistance. We acknowledge NIH/NIAID R21AI115136 (CAH) and R56AI121254 (CAH) for research support and CO6RR020135-01 for construction of the facility utilized for production and maintenance of MGH miniature swine.

References

- Avsar M, Jansson K, Sommer W, Kruse B, Thissen S, Dreckmann K, Knoefel AK, Salman J, Hafer C, Hecker J, Buechler G, Karstens JH, Jonigk D, Länger F, Kaever V, Falk CS, Hewicker-Trautwein M, Ungefroren H, Haverich A, Strüber M, Warnecke G. Augmentation of Transient Donor Cell Chimerism and Alloantigen-Specific Regulation of Lung Transplants in Miniature Swine. *Am J Transplant.* 2016; 16:1371. [PubMed: 26602894]

- Griesemer AD, Lamattina JC, Okumi M, Etter JD, Shimizu A, Sachs DH, Yamada K. Linked suppression across an MHC mismatched barrier in a miniature swine kidney transplantation model. *J Immunol.* 2008; 181:4027–4036. [PubMed: 18768858]
- Kaser T, Gerner W, Hammer SE, Patzl M, Saalmuller A. Phenotypic and functional characterisation of porcine CD4(+)CD25(high) regulatory T cells. *Vet Immunol Immunopathol.* 2008a; 122:153–158. [PubMed: 17868905]
- Kaser T, Gerner W, Hammer SE, Patzl M, Saalmuller A. Detection of Foxp3 protein expression in porcine T lymphocytes. *Vet Immunol Immunopathol.* 2008b; 125:92–101. [PubMed: 18565594]
- Kaser T, Gerner W, Saalmuller A. Porcine regulatory T cells: mechanisms and T-cell targets of suppression. *Dev Comp Immunol.* 2011; 35:1166–1172. [PubMed: 21530576]
- Kaser T, Mulleberner A, Hartl RT, Essler SE, Saalmuller A, Catharina Duvigneau J. Porcine T-helper and regulatory T cells exhibit versatile mRNA expression capabilities for cytokines and co-stimulatory molecules. *Cytokine.* 2012; 60:400–409. [PubMed: 22867872]
- Kaser T, Mair KH, Hammer SE, Gerner W, Saalmuller A. Natural and inducible Tregs in swine: Helios expression and functional properties. *Dev Comp Immunol.* 2015; 49:323–331. [PubMed: 25511662]
- Mayer CT, Ghorbani P, Köhl AA, Stüve P, Hegemann M, Berod L, Gershwin ME, Sparwasser T. Few Foxp3+ regulatory T cells are sufficient to protect adult mice from lethal autoimmunity. *Eur J Immunol.* 2014; 44:2990. [PubMed: 25042334]
- Molledo B, Hemmers S, Rudensky AY. Regulatory T cell ablation causes acute T cell lymphopenia. *PLoS One.* 2014; 9:e86762. [PubMed: 24466225]
- Peraino JS, Hermanrud CE, Springett L, Zhang H, Li G, Srinivasan S, Gusha A, Sachs DH, Huang CA, Wang Z. Expression and characterization of recombinant soluble porcine CD3 ectodomain molecules: mapping the epitope of an anti-porcine CD3 monoclonal antibody 89H2-6-15. *Cell Immunol.* 2012; 276:162. [PubMed: 22672968]
- Sugiyama D, Nishikawa H, Maeda Y, Nishioka M, Tanemura A, Katayama I, Ezoe S, Kanakura Y, Sato E, Fukumori Y, Karbach J, Jäger E, Sakaguchi S. Anti-CCR4 mAb selectively depletes effector-type FoxP3+CD4+ regulatory T cells, evoking antitumor immuneresponses in humans. *Proc Natl Acad Sci U S A.* 2013; 110:17945. [PubMed: 24127572]
- Talker SC, Kaser T, Reutner K, Sedlak C, Mair KH, Koinig H, et al. Phenotypic maturation of porcine NK- and T-cell subsets. *Dev Comp Immunol.* 2013; 40:51–68. [PubMed: 23352625]
- Wang Z, Duran-Struuck R, Crepeau R, Matar A, Hanekamp I, Srinivasan S, Neville DM Jr, Sachs DH, Huang CA. Development of a Diphtheria Toxin Based Antiporcine CD3 Recombinant Immunotoxin. *Bioconj Chem.* 2011; 22:2014. [PubMed: 21866954]
- Wang Z, Wei M, Zhang H, Chen H, Germana S, Huang CA, Madsen JC, Sachs DH, Wang Z. Diphtheria-toxin based anti-human CCR4 immunotoxin for targeting human CCR4(+) cells in vivo. *Mol Oncol.* 2015; 9:1458. [PubMed: 25958791]
- Wang Z, Pratts SG, Zhang H, Spencer PJ, Yu R, Tonsho M, Shah JA, Tanabe T, Powell HR, Huang CA, Madsen JC, Sachs DH, Wang Z. Treg depletion in non-human primates using a novel diphtheria toxin-based anti-human CCR4 immunotoxin. *Mol Oncol.* 2016; 10:553. [PubMed: 26643572]

Highlights

- Anti-human CCR4 immunotoxin binds to porcine leukocytes.
- Anti-human CCR4 immunotoxin effectively depletes CCR4⁺ Foxp3⁺ porcine Tregs *in vivo*.

Figure 1A

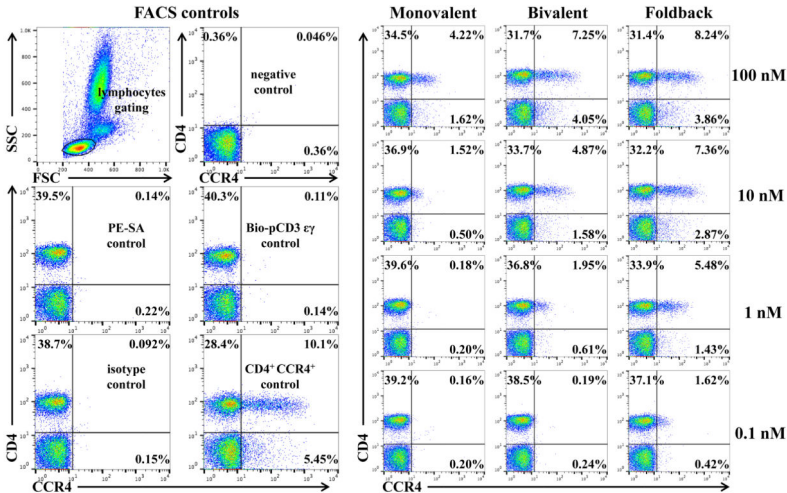


Figure 1B

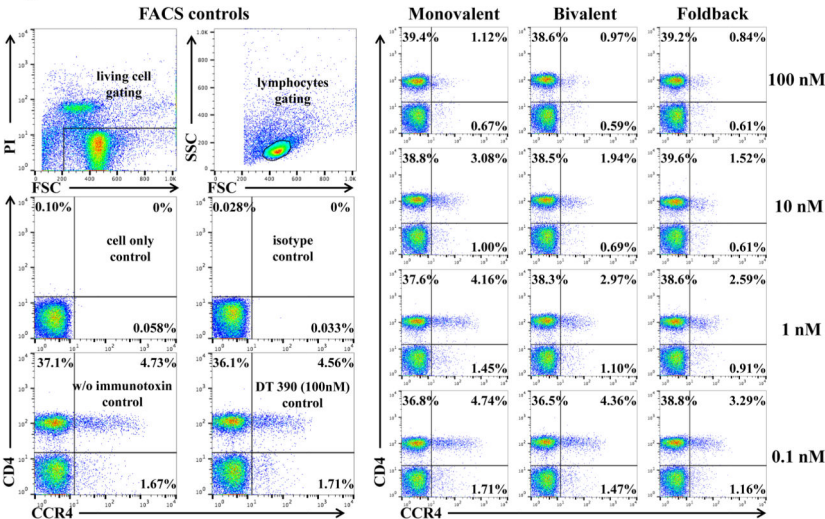
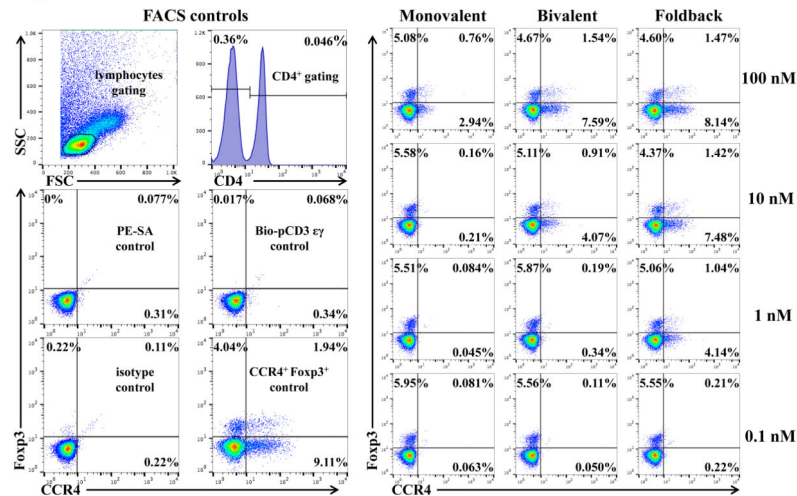


Figure 1C

**Fig. 1.**

In vitro binding and depletion analysis of the anti-human CCR4 immunotoxins to porcine CCR4⁺ blood cells or PBMC. **A)** Flow cytometry binding analysis of the anti-human CCR4 immunotoxins to CCR4⁺ cells within porcine whole blood. Monovalent: monovalent anti-human CCR4 immunotoxin [DT390-scFv (1567)]; Bivalent: bivalent anti-human CCR4 immunotoxin [DT390-BiscFv (1567)]; Foldback: single-chain foldback diabody anti-human CCR4 immunotoxin; PE-SA: PE-conjugated streptavidin; Bio-pCD3 $\epsilon\gamma$: Biotin-labeled porcine CD3 $\epsilon\gamma$. **B)** *In vitro* depletion of the CCR4⁺ cells within porcine PBMC using the anti-human CCR4 immunotoxins. **C)** Flow cytometry binding analysis of the anti-human CCR4 immunotoxins to the Foxp3⁺CCR4⁺ porcine PBMC. Fig. 1C analysis was CD4 gated. All of the data (Fig. 1A–C) are representative of three experiments with blood samples from three different animals. The variance data of Fig. 1A–C is included in the supplement table 1.

Figure 2A

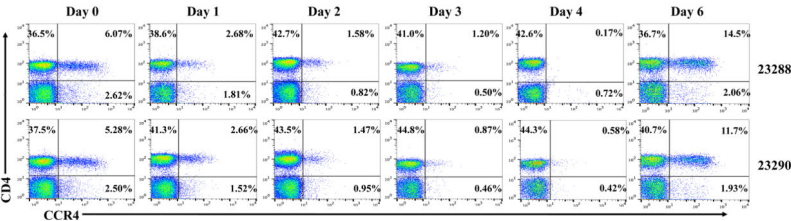


Figure 2B

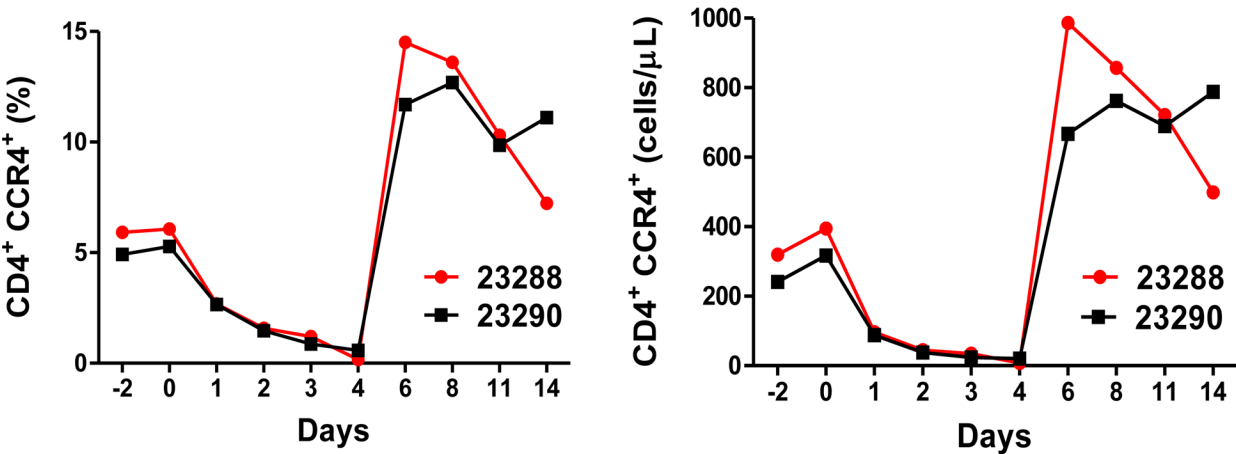


Figure 2C

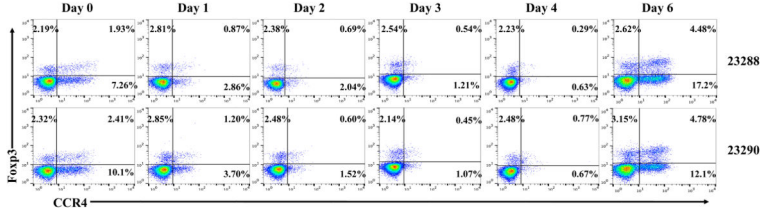


Figure 2D

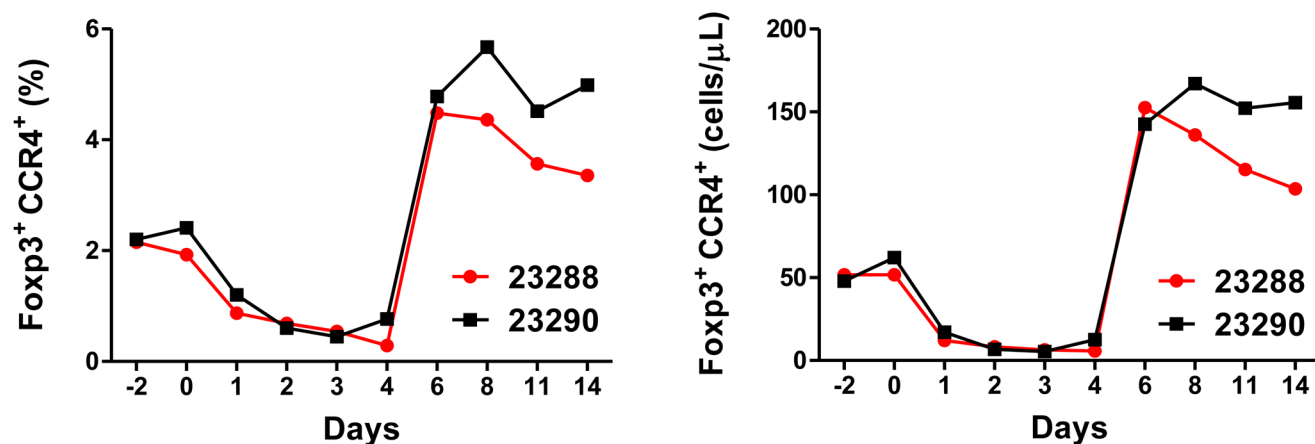


Figure 2E

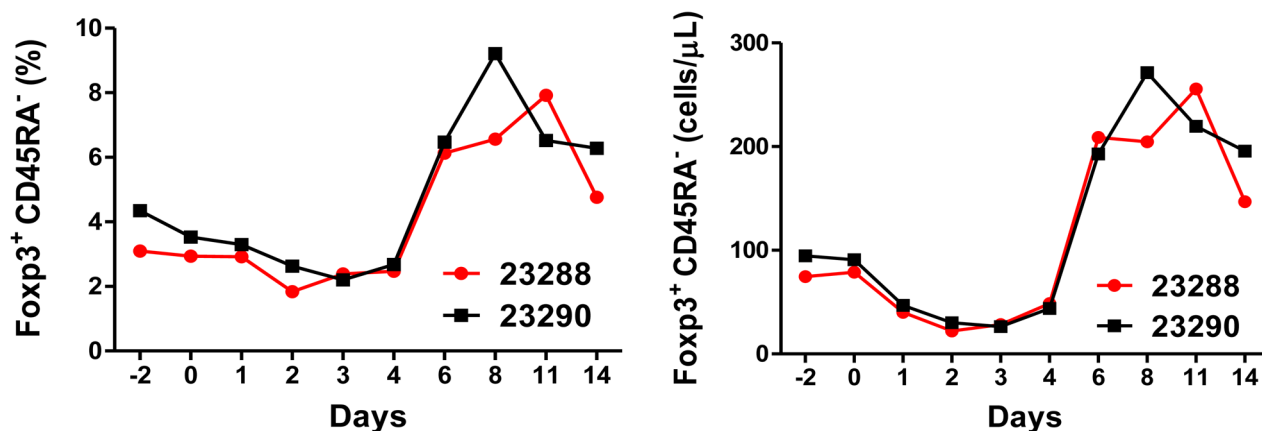


Figure 2F

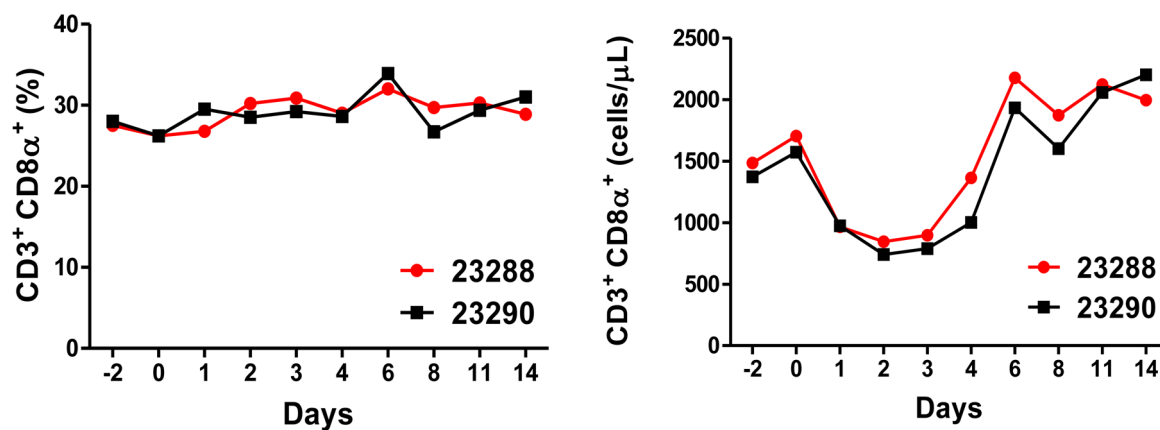


Figure 2G

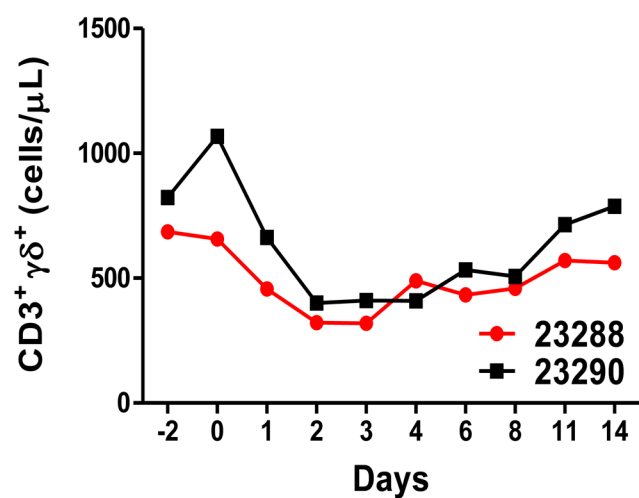
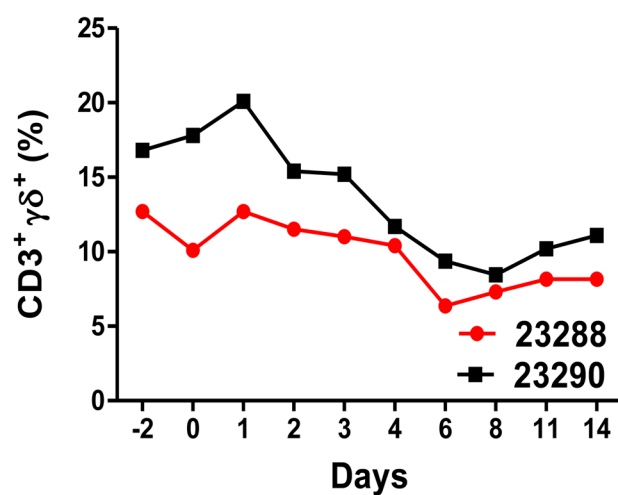


Figure 2H

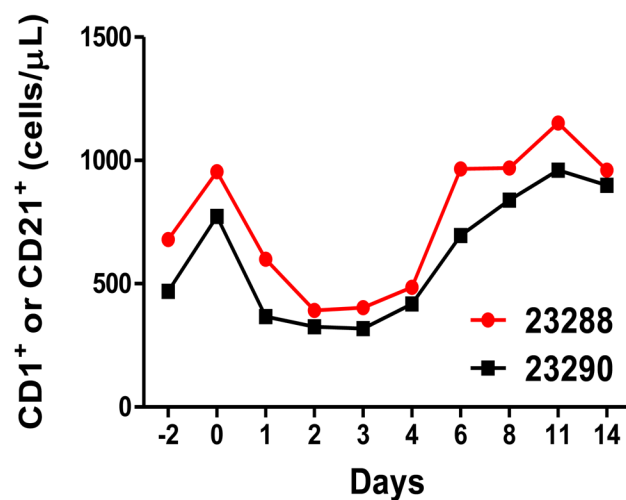
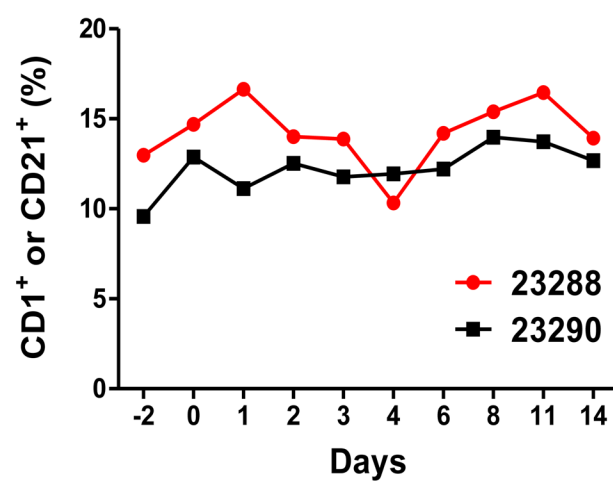


Figure 2I

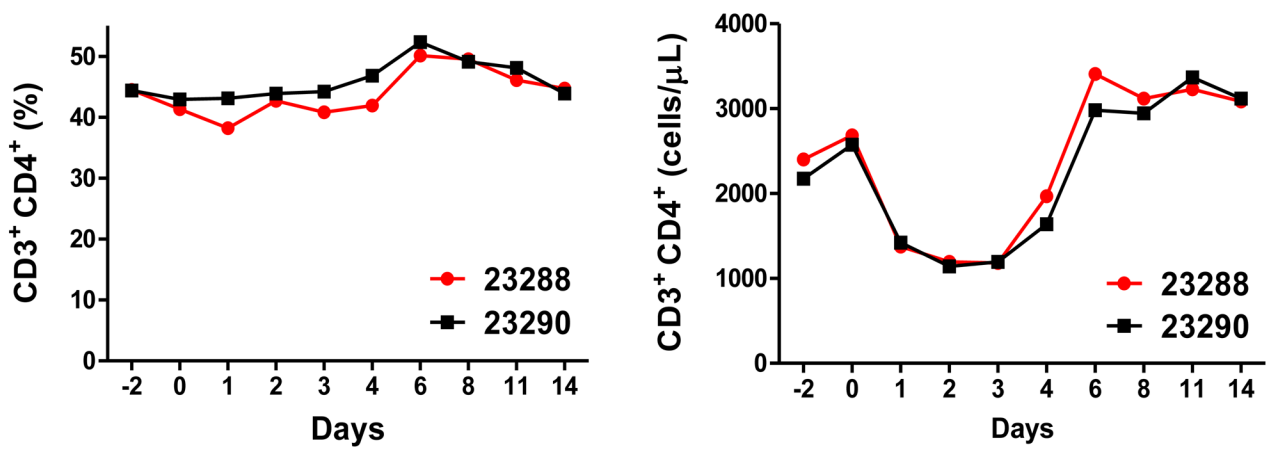


Figure 2J

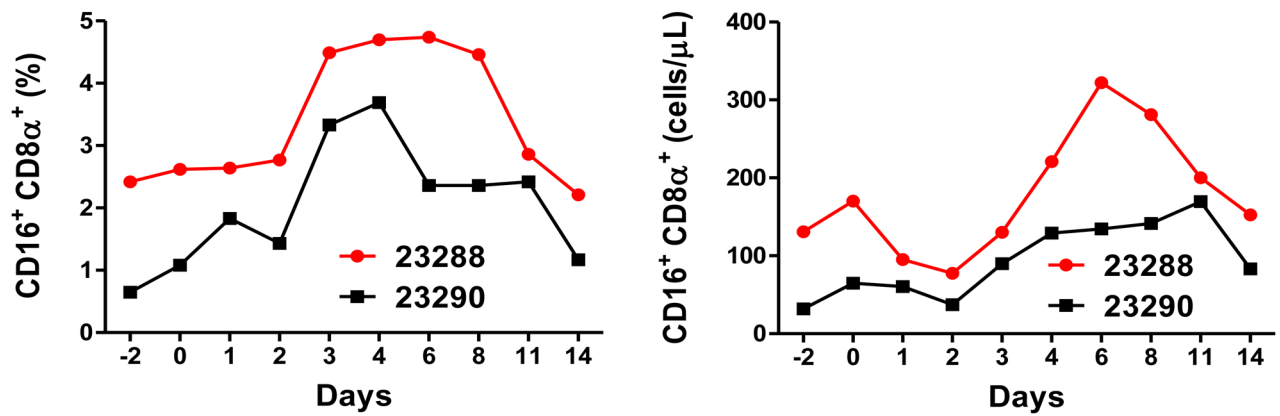


Figure 2K

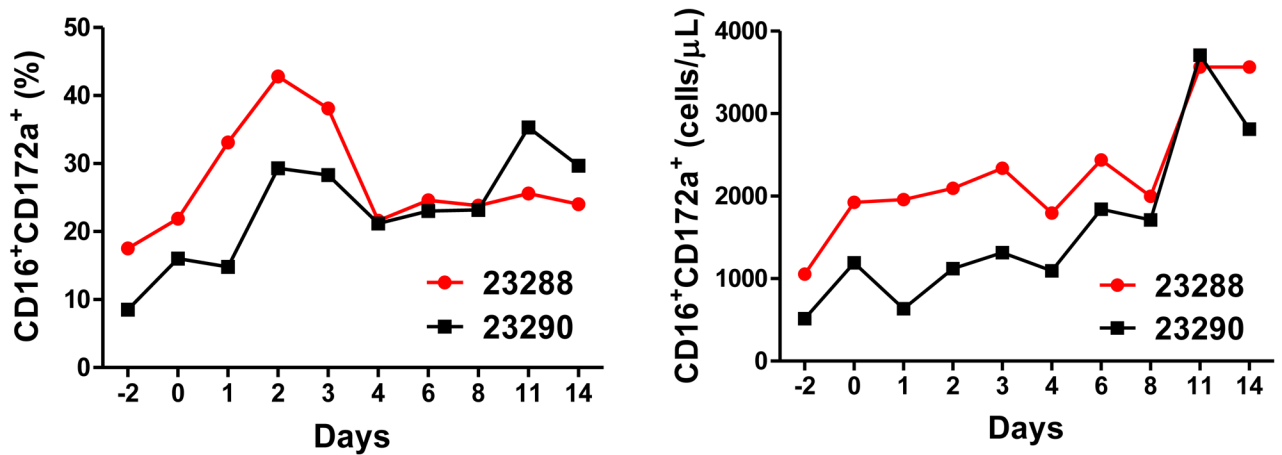


Figure 2L

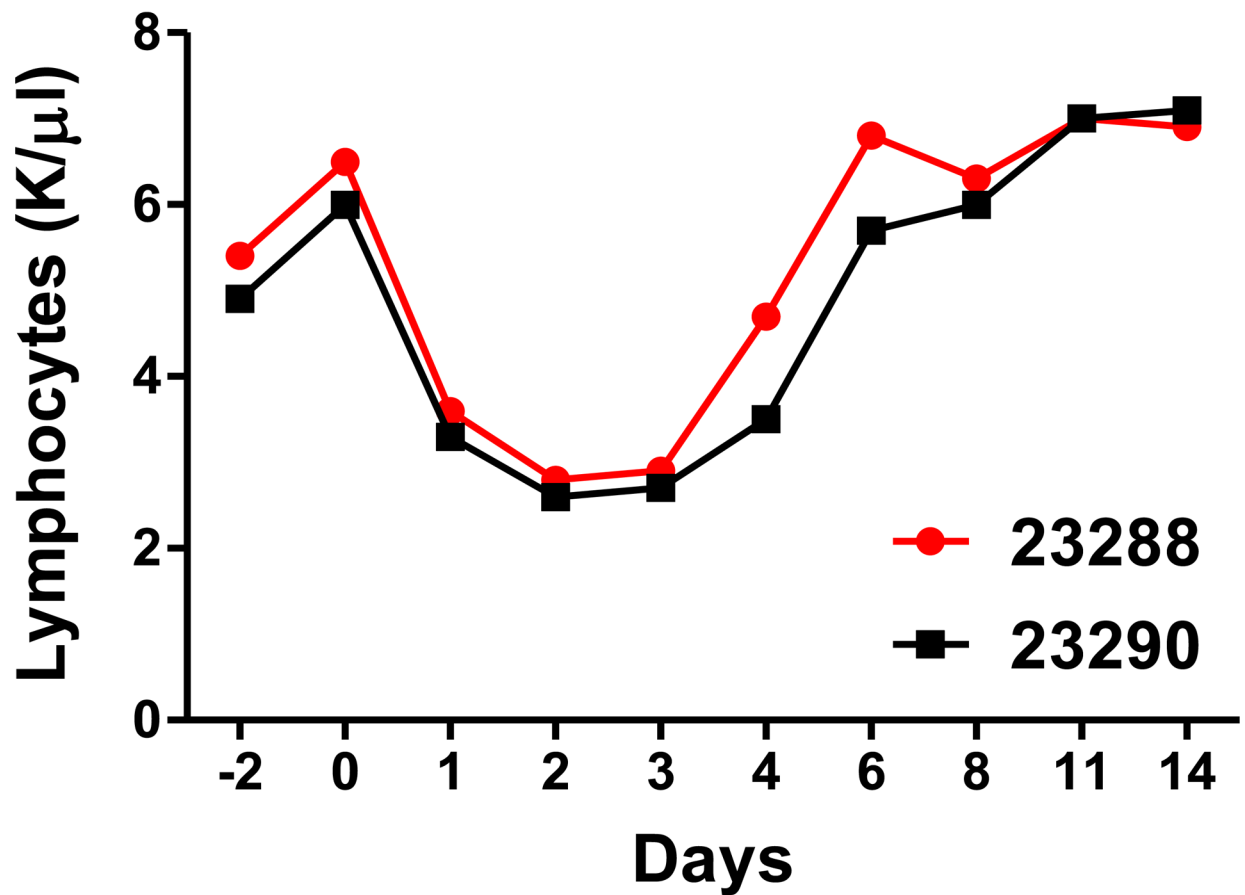


Fig. 2.

Porcine Treg depletion in the peripheral blood using the foldback diabody anti-human CCR4 immunotoxin. The immunotoxin was injected at 50 $\mu\text{g/kg}$ IV, BID for four consecutive days. Day 0 is the first day of the CCR4 immunotoxin administration. **A)** Representative flow cytometry analysis (day 0–4 and 6) of the CCR4⁺ cell depletion in the peripheral blood using the antibodies against CD4 and CCR4 (CD4⁺CCR4⁺). **B)** The CCR4⁺ cell depletion in the peripheral blood was monitored by flow cytometry using the antibodies against porcine CD4 and human CCR4 (CD4⁺CCR4⁺). **C)** Representative flow cytometry analysis (day 0–4 and 6) of the CCR4⁺Foxp3⁺ cell depletion in the peripheral blood using the antibodies against CCR4 and Foxp3 (CCR4⁺Foxp3⁺ among the gated CD4⁺ cells). **D)** The CCR4⁺Foxp3⁺ Treg depletion in the peripheral blood was monitored by flow cytometry using the antibodies against CCR4 and Foxp3 (CCR4⁺Foxp3⁺ among the gated CD4⁺ cells). **E)** The Foxp3⁺CD45RA⁻ effector Tregs in the peripheral blood were monitored by flow cytometry using antibodies against Foxp3 and CD45RA (Foxp3⁺CD45RA⁻). **F)** The CD8 α ⁺ T cells in the peripheral blood were monitored by flow cytometry using the antibodies against porcine CD3 and CD8 α (CD3⁺CD8 α ⁺). **G)** The $\gamma\delta$ ⁺ T cells in the peripheral blood were monitored by flow cytometry using antibodies against porcine CD3 and $\gamma\delta$ (CD3⁺ $\gamma\delta$ ⁺). **H)** The B cells (CD1⁺ or CD21⁺) in the peripheral blood were monitored by flow

cytometry using antibodies against porcine CD3 and porcine CD1 or human CD21 (CD3⁻CD1⁺ or CD3⁻CD21⁺). **I)** The CD4⁺ cells in the peripheral blood were monitored by flow cytometry using the antibodies against porcine CD3 and CD4 (CD3⁺CD4⁺). **J)** The CD8α⁺CD16⁺ NK cells in the peripheral blood were monitored by flow cytometry using antibodies against porcine CD8α and CD16 (CD8α⁺CD16⁺). **K)** The CD16⁺CD172a⁺ monocytes in the peripheral blood were monitored by flow cytometry using antibodies against porcine CD16 and CD172a (CD16⁺CD172a⁺, PBMC gating). **L)** The entire lymphocyte was monitored by complete blood count analysis using HESKA Veterinary Hematology System. Left panel (2B and 2D–K): percentage value curve; right panel (2B and 2D–K): absolute number curve.

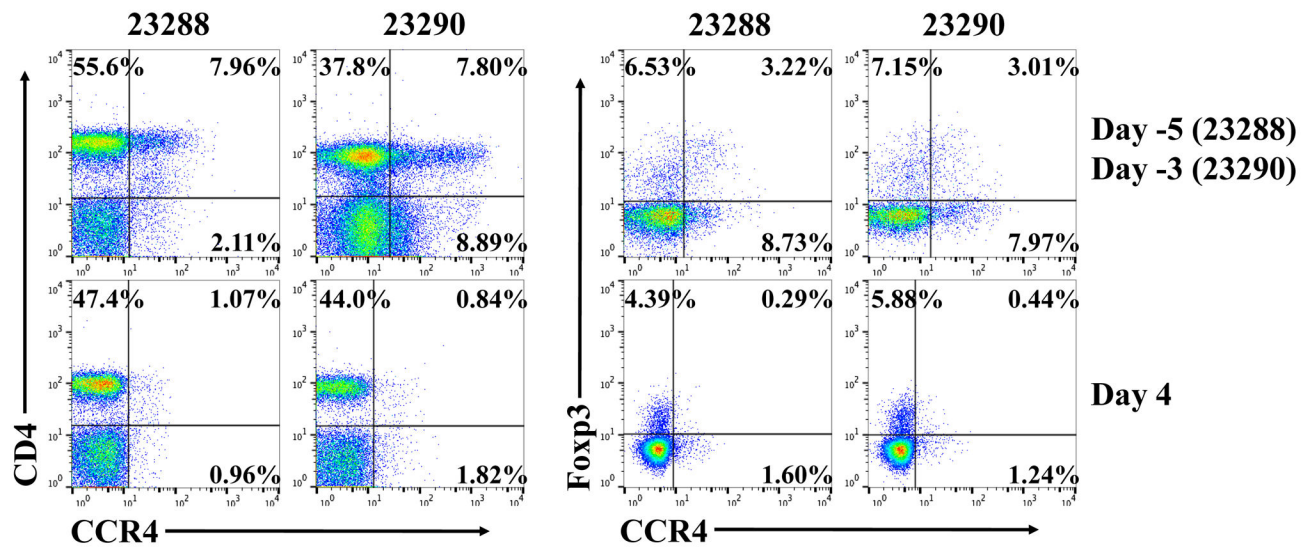
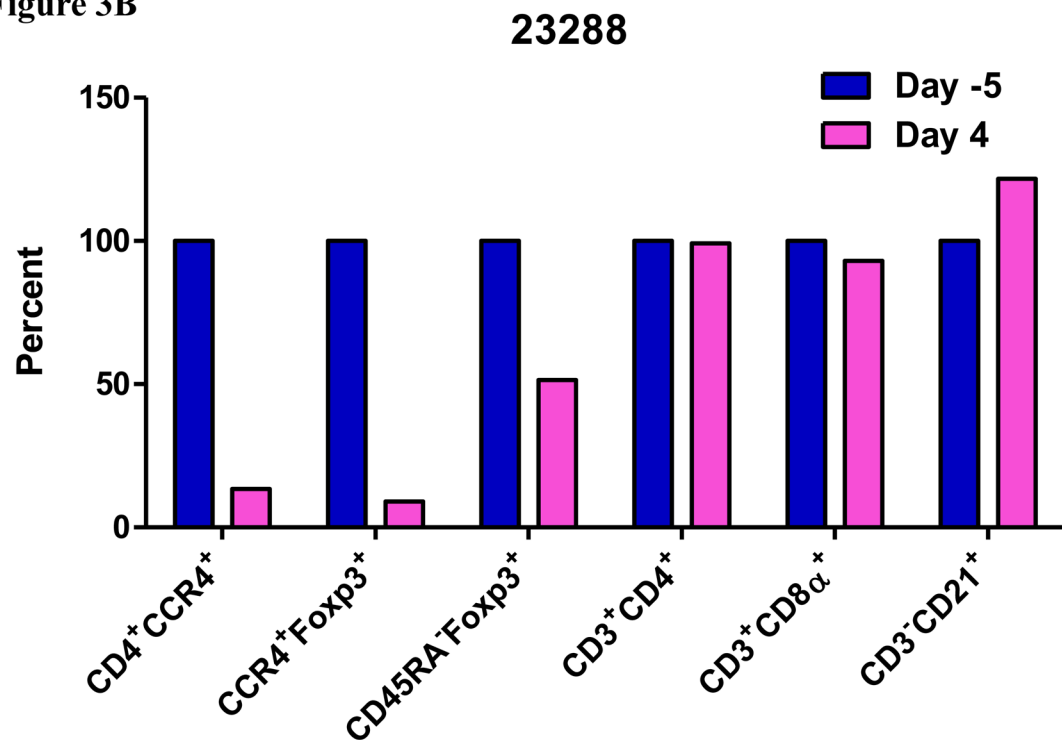
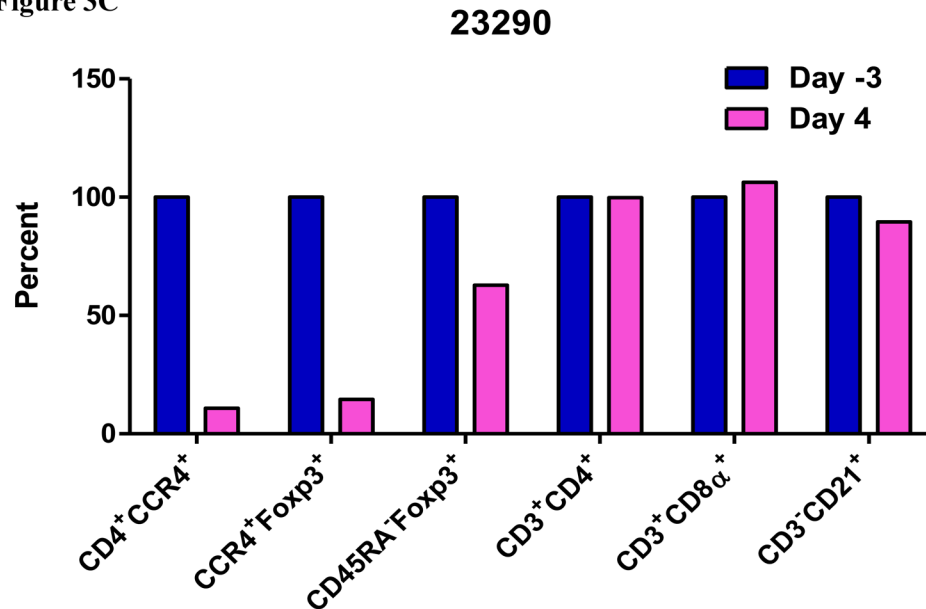
Figure 3A**Figure 3B**

Figure 3C

**Fig. 3.**

Porcine Treg depletion in the lymph nodes using the foldback diabody anti-human CCR4 immunotoxin. The lymph node biopsies were performed before the immunotoxin treatment on day -5 (Animal# 23288) or day -3 (Animal# 23290) and after the immunotoxin treatment on day 4. **A)** Representative flow cytometry analysis of the lymph node biopsy samples using antibodies against CD4, CCR4 and Foxp3 (CD4⁺CCR4⁺, CCR4⁺Foxp3⁺ among the gated CD4⁺ cells) before the immunotoxin treatment on day -5 (Animal# 23288) or day -3 (Animal# 23290) and after the immunotoxin treatment on day 4. **B–C)** The lymph node Treg depletion was monitored by flow cytometry using the antibodies against CD4, CCR4, CD45RA and Foxp3 (CCR4⁺ cells: CD4⁺CCR4⁺; CCR4⁺ Tregs: CCR4⁺Foxp3⁺ among the gated CD4⁺ cells; effector Tregs: CD45RA⁻Foxp3⁺ among the gated CD4⁺ cells). The other cell populations in lymph node were monitored by flow cytometry using antibodies against CD3, CD4, CD8α, CD21 (CD4⁺ T cells: CD3⁺CD4⁺; CD8α⁺ T cells: CD3⁺CD8α⁺; CD21⁺ B cells: CD3⁻CD21⁺).

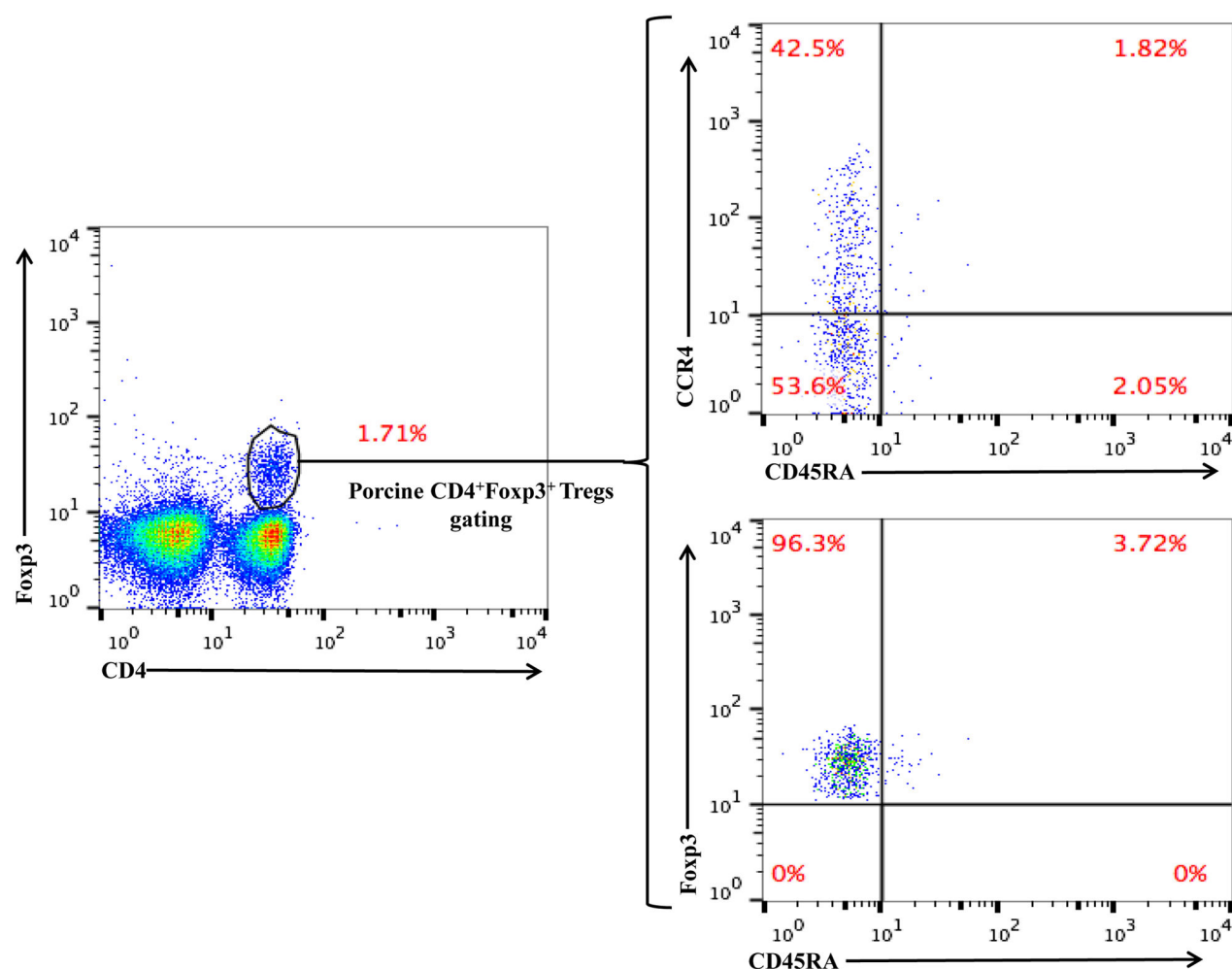


Fig. 4.

Flow cytometry analysis of the CCR4 versus CD45RA expression and Foxp3 versus CD45RA expression among the gated CD4⁺Foxp3⁺ porcine Tregs. The data are representative of two individual experiments with blood samples from two different animals.

Table 1

Antibodies used in this study

Antibody Name	Clone#	Source	Cat#
FITC- mouse anti-pig CD1	76-7-4	In house	
FITC-mouse anti-pig CD3	898H-2-6-15	In house	
FITC-mouse anti-pig CD4a	74-12-4	In house	
FITC-mouse anti-pig CD45RA	Fg2F9	In house	
Biotin-mouse anti-pig CD45RA	Fg2F9	In house	
FITC-mouse anti-pig CD16	G7	In house	
PerCp-Cy5.5-mouse anti-pig CD4a	74-12-4	BD Bioscience	561474
PE-mouse anti-pig CD8a	76-2-11	BD Bioscience	559584
Alexa Fluor® 647-mouse anti pig CD8a	76-2-11	BD Bioscience	561475
PE-mouse anti-human CD21	B-ly4	BD Bioscience	555422
PE-rat anti-pig $\gamma\delta$ T lymphocytes	MAC320	BD Bioscience	561486
PE-mouse anti-pig CD172a	74-22-15A	BD Bioscience	561499
PE-mouse IgG 2b κ	MPC-11	BD Bioscience	559529
Fluorescein-mouse anti-human/rat CCR4	205410	R&D Systems	FAB1567F
PE-mouse anti-human/rat CCR4	205410	R&D Systems	FAB1567P
Mouse IgG2B fluorescein isotype control	133303	R&D Systems	IC0041F
PE-mouse anti-human CD194 (CCR4)	L291H4	BioLegend	359412
PE-mouse IgG1, κ isotype control	MOPC-21	BioLegend	400139
PE-streptavidin		BioLegend	405204
APC-streptavidin		Biolegend	405207
FITC-rat anti-mouse Foxp3	FJK-16s	eBioscience	11-5773-82
FITC-rat IgG2a, κ isotype control	eBR2a	eBioscience	11-4321-42
Propidium Iodide		Sigma	81845
7-Aminoactinomycin (7-AAD)		Sigma	A9400